Photoexcited Small Polaron Formation in Goethite (α-FeOOH) Nanorods Probed by Transient Extreme Ultraviolet Spectroscopy

Ilana J. Porter[†,‡], Scott K. Cushing[†,‡], Lucas M. Carneiro[†,‡], Angela Lee[†], Justin C. Ondry[†,§], Jakob C. Dahl[†,§], Hung-Tzu Chang[†], A. Paul Alivisatos[†,§,⊥,‖], Stephen R. Leone[†,‡,∇,]*

† Department of Chemistry, University of California, Berkeley, California 94720, United States

‡ Chemical Sciences Division, Lawrence Berkeley National Laboratory, Berkeley, California 94720, United States

§ Materials Sciences Division, Lawrence Berkeley National Laboratory, Berkeley, California 94720, United States

⊥ Department of Materials Science and Engineering, University of California, Berkeley, California 94720, United States

‖ Kavli Energy NanoScience Institute, Berkeley, California 94720, United States

∇ Department of Physics, University of California, Berkeley, California 94720, United States

Corresponding Author

*e-mail: srl@berkeley.edu

1. Extreme Ultra-Violet (XUV) Transient Absorption Spectra

Pulses that are 40 fs, 3.5 mJ centered at 800 nm are produced by a 1 kHz Ti:sapphire chirped pulse amplifier (Spitfire Pro, Spectra Physics). The XUV probe pulse is generated via high harmonic generation in a semi-infinite gas cell (40 cm) filled with 110 Torr (approximately 1.4×10^4 Pascal) neon gas. Before the gas cell, a portion of the 800 nm light is converted to 400 nm using in-line second harmonic generation, allowing for the production of both odd- and even-order harmonics.[1] A 0.5 mm thick glass capillary array (pore size 5 μm) blocks the 800 nm and 400 nm fundamental before the sample while transmitting the XUV.[2] The XUV spot size is 200 μm at the sample. After the sample, the XUV pulses are spectrally dispersed using a variable line spacing grating, which has an energy range of 35 eV-110 eV. The dispersed spectrum at each time delay is captured by a charge-coupled device (CCD) camera (PIXIS-400, Princeton Instruments).

The pump pulses are generated by passing a portion of the 800 nm beam through an optical parametric amplifier (TOPAS-Prime, Light Conversion) to create visible pulses with tunable wavelength (2.2 – 3.1 eV, 560 – 400 nm). The pump spot size is approximately 400 μm at the sample with a power density of approximately 2 mJ. Each transient spectrum consists of 200 scans that are averaged together, each consisting of 61 time delays spaced logarithmically after time zero (-2500 fs to +300 ps about time zero, delay steps ranging from 14 fs to 25 ps). Each time delay comprises a pump-on and a pump-off camera image of XUV light versus photon energy produced from the coaddition of approximately 800 pulses. To avoid thermal damage and ablation, the samples are raster scanned in 100 μm steps between each pump-probe time delay. Additionally, a stream of dry nitrogen is flowed over the sample to dissipate heat.

2. Sample Fabrication

Goethite, or iron (III) oxide hydroxide (FeOOH), nanorods of dimensions ranging from 5 nm x 20 nm to 30 nm x 150 nm were purchased from U.S. Research Nanomaterials, Inc. and spun-cast onto 30 nm thick 3 mm x 3 mm Si_3N_4 substrates (3 mg of FeOOH in 30 μL Millipore water, spun for 60 s, 2000 rpm). This affords an uneven-density film, and measurements are taken on a portion exhibiting the same XUV absorbance as a 35 nm thin film (from comparison to CXRO transmission).[3]

3. Sample Characterization

a) TEM imaging TEM and HRTEM imaging is performed with a FEI Tecnai T20 S-TWIN TEM operating at 200 kV with a LaB_6 filament, which affords a resolving power of 2.4 Å. TEM images are collected with a Gatan Orius SC200 TEM camera with a 1 second exposure time to capture the rod-like shapes (Figure 1b, main text). High resolution images are taken near the Scherzer focus without the use of an objective aperture in order to resolve the lattice fringes (Figure 1c, main text).

b) Powder X-Ray Diffraction Powder diffraction patterns of nanocrystalline samples (Figure 1d, main text) are obtained using a Bruker D-8 GADDS diffractometer equipped with a Co Kα source. XRD was collected in reflection geometry with an incident x-ray angle (ω) of 15°. Samples were prepared by drop casting a concentrated solution of nanocrystals in ethanol on an amorphous plastic low background substrate. 2D patterns were merged and integrated in the DIFFRAC.EVA software from Bruker.

4. Charge Transfer Multiplet Modeling of the Ground State

The ground state absorption spectrum is predicted using a charge transfer multiplet calculation performed with the CTM4XAS software.[4] The ground state calculation was conducted for the Fe^{3+}

oxidation state of iron. To include the effect of shorter Auger lifetimes at higher energies, the predicted spectra are broadened by a Lorentzian with a nominal width of 0.1 eV at 52 eV that linearly increases by 1 eV for every 1.5 eV and with a Fano asymmetry parameter of 3.5. Additionally, a Gaussian of width 0.5 eV is applied to account for the instrument response. An energetic shift of +1.7 eV to the absolute energy of the transitions is required.[5] A nonlinear fit was performed on the ground state absorption spectrum to determine the value of 10Dq, using the simulated spectra discussed above as model data. The value of 10Dq was found to be 1.55 eV ± 0.01 eV. The simulated ground state spectrum shown in Figure 1a in the main text uses a 10Dq value of 1.55 eV, with broadenings discussed above.

5. Charge Transfer Multiplet Modeling of the Excited State Differential Absorption

a) Charge-Transfer Hybridized State The XUV differential absorption for the optically excited state was predicted by subtracting the ground state absorption spectrum from the excited state spectrum predicted by a charge transfer multiplet calculation. The optically induced charge transfer from the oxygen site to the iron center is accounted for by setting the final oxidation state to be Fe^{2+} and considering only the lowest energy $^5T_1$ transition.[5,6] The calculation is otherwise performed as outlined in Section 4.

b) Polaron State The XUV differential absorption of the polaron state, which remains 20 ps after optical excitation, was predicted by subtracting the ground state absorption spectrum from the modeled polaron state spectrum. The polaron state is modeled as a splitting of the 3p core level into three states, using the splitting values and weightings for the Fe^{3+} center theoretically predicted for $FePO_4$[7] and experimentally found accurate for hematite[6]. Specifically, the measured ground state absorption spectrum is convolved with three delta functions spaced at 0 eV, 1 eV, and 2.5 eV

and with weightings of 1/3, 1/2, and 1/6, respectively. No additional shifting or broadening was applied.

6. Polaron Formation Kinetic Model

The kinetic model for the polaron formation includes a two-temperature model for the electron-phonon equilibrium and a bimolecular kinetic term for the recombination of the electron and phonon to form the polaron. In a standard two-temperature model, first a nonthermal electron population is created by optical excitation. Subsequently, electron-phonon scattering thermalizes the hot electrons while creating a nonthermal phonon population. The energy transfer rate between these two populations depends on their relative temperature and the electron-phonon scattering time, τ_{e-ph}. Thus, the predicted excited state temperature gives a measure of the average state occupations.

Since there is no clear relationship between temperature of the hot electrons and the measured amplitude of the charge-transfer hybridized state, average population is used in this model in place of temperature. An amplitude accounting for the unknown ratio of population transfer between hot electrons and phonons is then left as an additional fit parameter. In equations (1) and (2) below, the average hot electron population is denoted as η_e and the average hot phonon population is η_{ph}. The fit amplitude is denoted as A_e.

$$\dot{\eta}_e = -\frac{A_e \cdot \eta_e - \eta_{ph}}{\tau_{e-ph}} \quad (1)$$

$$\dot{\eta}_{ph} = \frac{A_e \cdot \eta_e - \eta_{ph}}{\tau_{e-ph}} \quad (2)$$

The second part of the polaron formation kinetic model is the bimolecular recombination of an electron and optical phonon, which also uses average population. This bimolecular term involves both the electron and phonon populations and the polaron formation time, τ_{pol}. This creates a

population of polarons, denoted as η_{pol} in equations (3), (4), and (5). An additional polaron population transfer amplitude, A_{pol}, is included to account for the unknown number of phonon scattering processes that occur during polaron formation.

$$\dot{\eta}_e = -\frac{A_e \cdot \eta_e - \eta_{ph}}{\tau_{e-ph}} - \frac{A_{pol} \cdot \eta_e \cdot \eta_{ph}}{\tau_{pol}} \quad (3)$$

$$\dot{\eta}_{ph} = \frac{A_e \cdot \eta_e - \eta_{ph}}{\tau_{e-ph}} - \frac{A_{pol} \cdot \eta_e \cdot \eta_{ph}}{\tau_{pol}} \quad (4)$$

$$\dot{\eta}_{pol} = \frac{A_{pol} \cdot \eta_e \cdot \eta_{ph}}{\tau_{pol}} \quad (5)$$

Fitting the multivariate regression of the experimental data with this model yields the electron-phonon scattering time, the polaron formation time, and two amplitude coefficients. These amplitudes not only account for the unknown ratios between populations, they also link the predicted hot electron and polaron populations from this model to the experimental differential absorption intensities of the charge-transfer hybridized state and the polaron state, respectively. The polaron formation probability is taken as the ratio of these fit amplitudes. It is important to note that this model is only valid when the polaron formation is complete by the end of electron thermalization, as the electron population in the model is depleted after thermalization. This approximation is justified here because the measured polaron feature reaches a maximum in a few picoseconds, the same time scale as thermalization.

The electron-phonon scattering time is found to be less than 30 fs at all four excitation energies studied. Since this is within the instrument response, this variable was held constant at 30 fs for all four fits. Fixing this variable in the fit did not change the results of the other three variables within error. Results are shown below in Table S1.

Table S1. Parameters of the Polaron Kinetic Model Fit at the Four Pump Photon Energies.

Excitation Photon Energy (eV)	Polaron Formation Time (fs)	Charge-Transfer Hybridized State Amplitude	Polaron State Amplitude
3.1	215 ± 20	2.0 ± 0.2	1.85 ± 0.01
2.6	350 ± 30	1.7 ± 0.1	1.49 ± 0.02
2.4	110 ± 35	2.0 ± 0.5	1.81 ± 0.08
2.2	70 ± 10	3.6 ± 0.4	2.45 ± 0.02

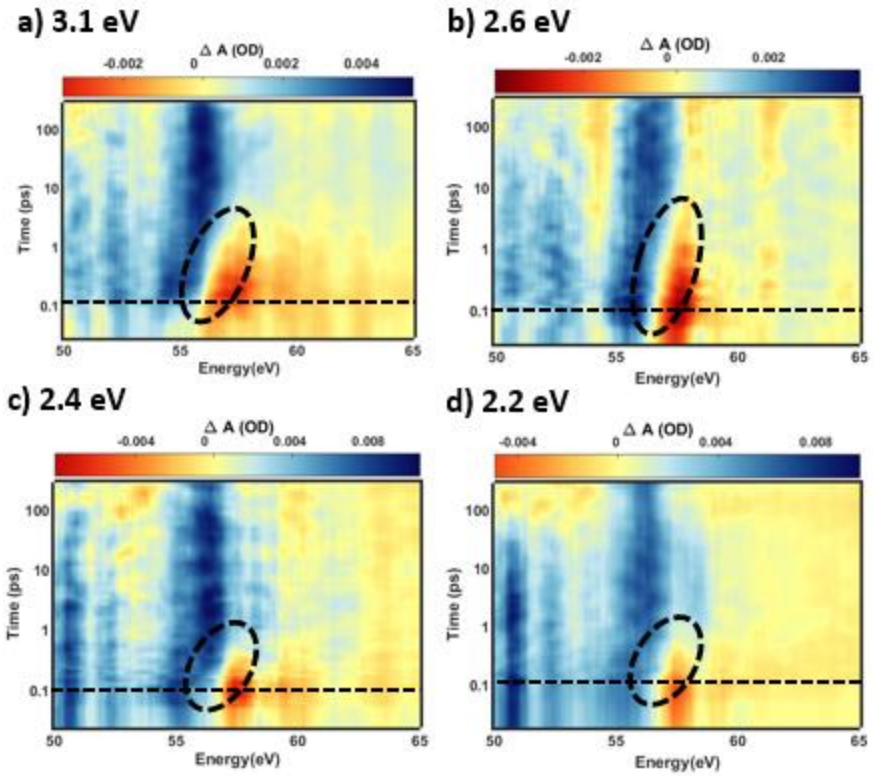

Figure S1. Transient absorption spectra of the nanorods pumped at different photon energies. All four spectra show the zero-crossing shift from approximately 56 eV to 57 - 59 eV within the first 2 ps, indicated by the thick dotted black oval. The thin horizontal dotted black line indicates time zero, which is offset my 100 fs to improve the clarity of the plot.

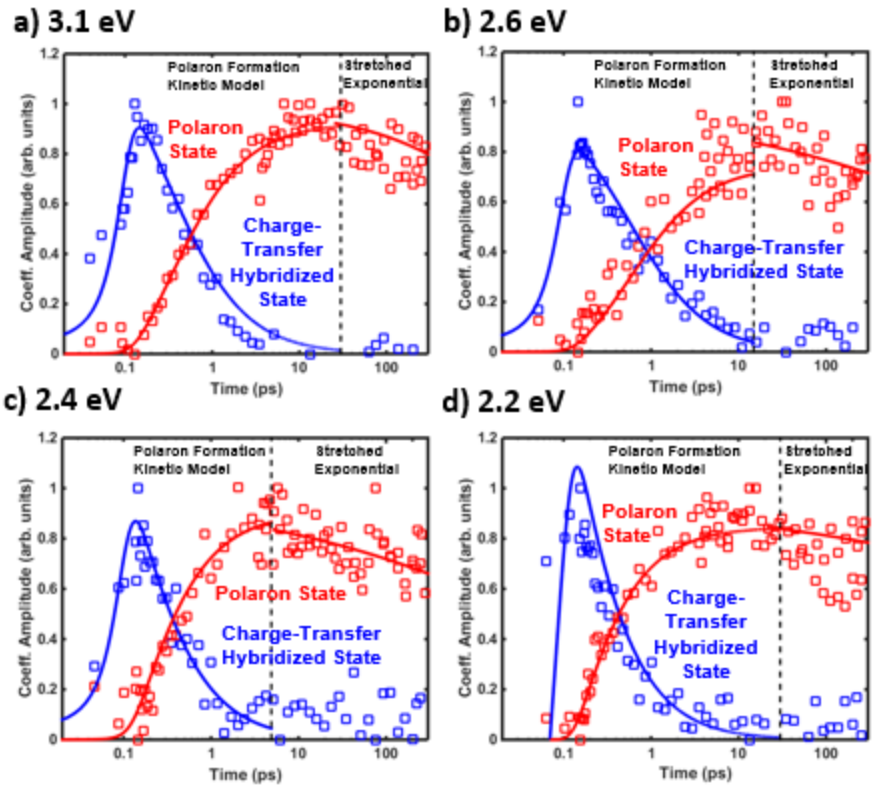

Figure S2. Amplitudes of the multivariate regression are shown at different pump wavelengths for the charge-transfer hybridized state (blue squares) and polaron state (red squares) with time on a logarithmic scale. For short times before the black dotted line, the fit using the polaron kinetic model is shown as solid lines. At long times, the fit using the stretched exponential decay model is shown. This long-time fit is inaccurate and does not match up with the short-time fit, as can be seen clearly in the 2.6 eV plot. The fitted polaron formation times are 215 ± 20 fs for 3.1 eV excitation, 350 ± 30 fs for 2.6 eV excitation, 110 ± 35 fs for 2.4 eV excitation, and 70 ± 10 fs for 2.2 eV excitation.

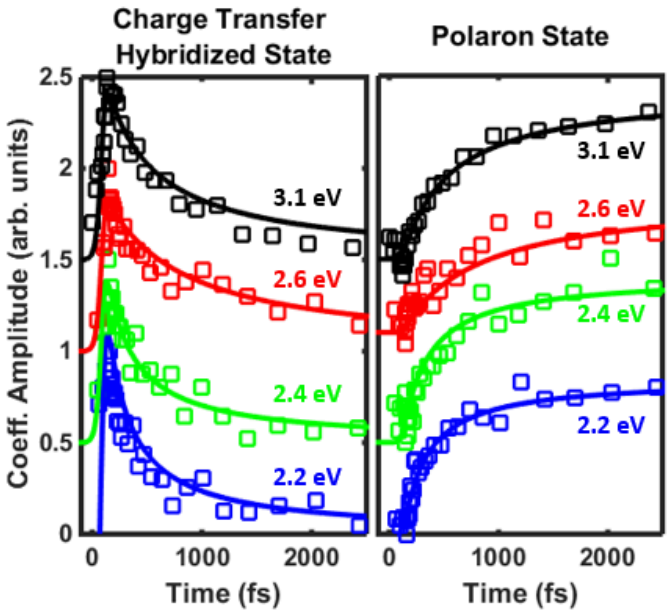

Figure S3. Amplitudes of the multivariate regression (squares) with the fit using the polaron kinetic model (solid lines) compared between the different pump photon energies. The amplitudes of the charge-transfer hybridized state are on the left, and the amplitudes of the polaron state are on the right. Results are shown with a linear time axis. A constant vertical offset is applied to the different pump wavelengths for clarity.

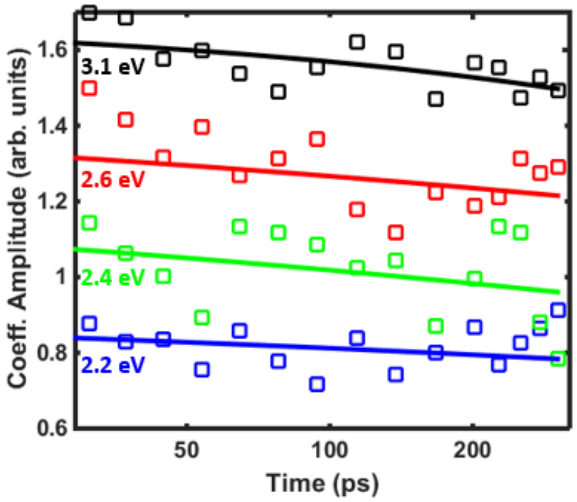

Figure S4. The decay of the polaron state, fit using the stretched exponential model. The multivariate regression amplitudes of the polaron state are shown as squares. The best fit using a stretched exponential is shown as solid lines. Results are shown with a logarithmic time axis. A constant vertical offset is applied to the different pump wavelengths for clarity.

REFERENCES

(1) Kfir, O.; Bordo, E.; Haham, G. I.; Lahav, O.; Fleischer, A.; Cohen, O. In-line Production of a Bi-circular Field for Generation of Helically Polarized High-Order Harmonics. *Appl. Phys. Lett.* **2016**, *108*, 211106.

(2) Zhang, Q.; Zhao, K.; Li, J.; Chini, M.; Cheng, Y.; Wu, Y.; Cunningham, E.; Chang, Z. Suppression of Driving Laser in High Harmonic Generation with a Microchannel Plate. *Opt. Lett*. **2014**, *39* (12), 3670-3673.

(3) Henke, B. L.; Gullikson, E. M.; Davis, J. C. X-Ray Interactions: Photoabsorption, Scattering, Transmission, and Reflection at E=50-30000 eV, Z=1-92. *At. Data Nucl. Data Tables* **1993**, *54* (2), 181-342.

(4) Stavitski, E.; de Groot, F. M. F. The CTM4XAS Program for EELS and XAS Spectral Shape Analysis of Transition Metal L Edges. *Micron*. **2010**, *41*, 687-694.

(5) Vura-Weis, J.; Jiang, C.-M.; Liu, C.; Gao, H.; Lucas, J. M.; de Groot, F. M. F.; Yang, P.; Alivisatos, A. P.; Leone, S. R. Femtosecond $M_{2,3}$-Edge Spectroscopy of Transition-Metal Oxides: Photoinduced Oxidation State Change in α-Fe_2O_3. *J. Phys. Chem. Lett*. **2013**, *4*, 3667–3671.

(6) Carneiro, L. M.; Cushing, S. K.; Liu, C.; Su, Y.; Yang, P.; Alivisatos, A. P.; Leone, S. R. Excitation-Wavelength-Dependent Small Polaron Trapping of Photoexcited Carriers in α-Fe2O3. *Nat. Mater.* **2017**, *16*, 819-825.

(7) Wang, Z.; Bevan, K. H. Exploring the Impact of Semicore Level Electronic Relaxation on Polaron Dynamics: An Adiabatic Ab Initio Study of FePO4. *Phys. Rev. B* **2016**, *93*, 024303.